Turbulence Ingestion Noise from an Open Rotor with Different Inflows

W. Nathan Alexander, William J. Devenport, Nicholas J. Molinaro, N. Agastya Balantrapu, Christopher Hickling, Stewart A. L. Glegg and Jack Pectol

Abstract Measurements have been performed on a scaled version of a Sevik rotor ingesting both a planar turbulent wake and a turbulent boundary layer flow. In both cases, detailed measurements were made of the inflow turbulence, including three-component turbulence profiles and the full cross-sectional 4-dimensional space-time correlation function. Far-field sound measurements were also made of the turbulence ingestion noise for a comprehensive range of rotor advance ratios varying from zero to high thrust, for rotor yaw angles out of the plane of the wake from −15 to 15°, and for a range of wake strike positions on the rotor disk. Probes mounted on two of the rotor blades were used to measure upwash fluctuations seen in the rotating frame, as well as blade-to-blade coherence spectra. Comparisons have been made with predictions of the far-field sound levels based on the measured inflow turbulence for both configurations and good results were obtained in all cases.

Keywords Aeroacoustics · Rotor noise · Turbulence ingestion

1 Introduction

Sound radiation from rotors operating in turbulent flow has been studied extensively following the pioneering work of Sevik [1] in the water tunnel at Penn State. Sevik measured the unsteady loading on a rotor operating in a homogeneous turbulent flow downstream of a rectangular grid. He also outlined a procedure to predict the unsteady loading and the radiated sound from the rotor based on the wavenumber spectrum of the turbulent inflow. This problem has been reconsidered many times over the years since Sevik's early experiment and, with suitable modifications to Sevik's theory, rotor noise caused by homogeneous or quasi-homogeneous turbulent

W. N. Alexander · W. J. Devenport (✉) · N. J. Molinaro · N. A. Balantrapu · C. Hickling
Center for Renewable Energy and Aerodynamic Technology, Virginia Tech, Blacksburg, VA, USA
e-mail: Devenport@vt.edu

S. A. L. Glegg · J. Pectol
Florida Atlantic University, Boca Raton, FL, USA

E. Ciappi et al. (eds.), *Flinovia—Flow Induced Noise and Vibration Issues and Aspects-II*,
https://doi.org/10.1007/978-3-319-76780-2_8

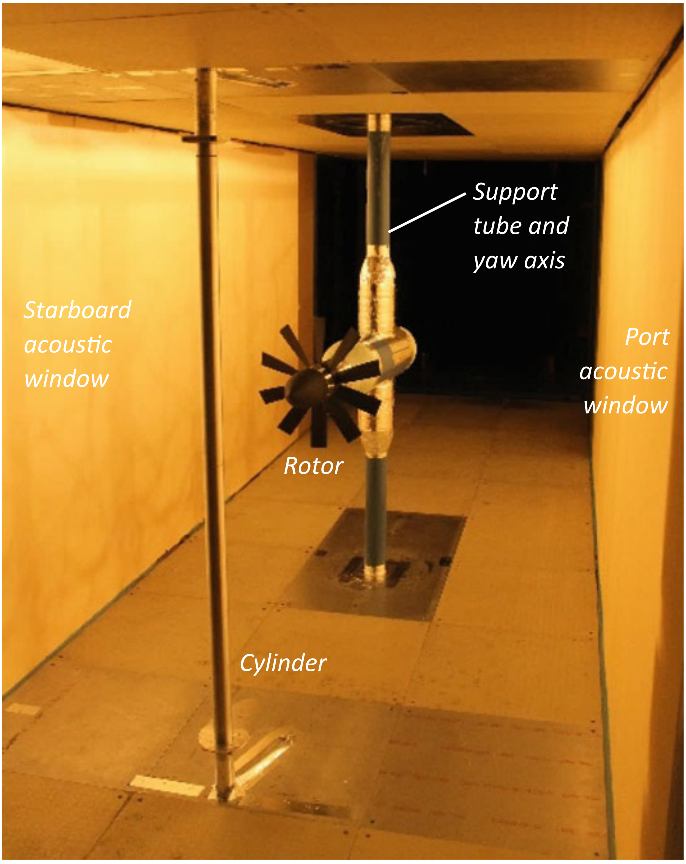

Fig. 1 Cylinder and rotor mounted in the anechoic section of the Virginia Tech Stability Wind Tunnel

inflows is well understood, providing that the wavenumber spectrum of the turbulent inflow can be suitably modeled, and turbulence lengthscales estimated using rapid distortion theory (RDT). Example studies have been completed on helicopter rotors, wind turbines, and fans operating in a duct wall boundary layer as well as in grid turbulence [2–8]. However, the problem of an inhomogeneous turbulent inflow, for which the wavenumber spectrum of the flow is undefined, has received less attention. Over the last few years, a series of theoretical, experimental, and numerical studies have been carried out to advance the understanding of this problem by specifically considering the sound radiation from a rotor that is in the wake of a cylinder (Fig. 1) or placed close to a flat wall so it ingests the wall boundary layer over a limited part of the rotor disk plane (Fig. 2). In this paper, we will review these studies and summarize the similarities and differences between the two sets of inflow conditions.

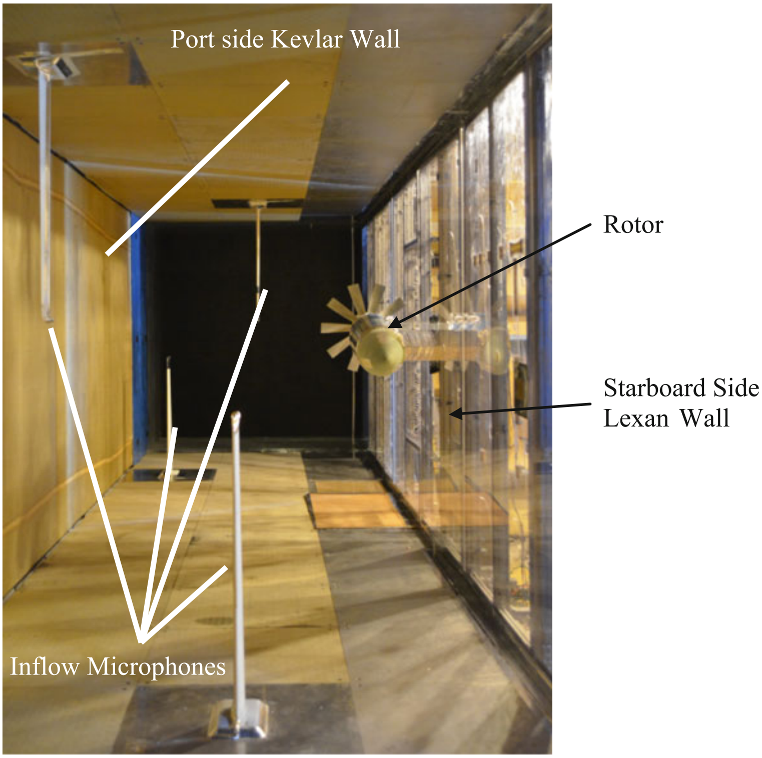

Fig. 2 Rotor mounted near a wall in the Virginia Tech Stability Wind Tunnel

The initial work focused on the ingestion of a thick planar turbulent wall boundary layer by a rotor next to a wall as shown in Fig. 2. Morton et al. [9] documented the complete cross-sectional space-time correlation of this flow to serve as the inflow boundary condition. Alexander et al. [10], Wisda et al. [11, 12], and Murray et al. [13] examined the rotor sound field. Alexander et al. [14] presented direct measurement of two-point blade-to-blade upwash correlations in the rotating frame, and Glegg et al. [15, 16] made predictions of the rotor noise based on the measured inflow correlations. The broadband spectra were found to be predictable for low and moderate thrust cases but at high thrust the experimental measurements of the far-field sound showed the spectral peaks becoming almost tonal and this will be discussed in more detail in Sect. 3.

Following the initial study, a second set of experiments were carried out [17] to investigate the sound produced by the rotor when it ingested a wake shed from a cylinder located upstream of the rotor (Fig. 1). As described below, the results from these two experiments show substantial differences that can be related to the details of the inflow turbulence.

2 The Rotor Systems and the Wind Tunnel

Measurements were performed in the hybrid anechoic test section of the Virginia Tech Stability Wind Tunnel [18]. Sound generated in the test section radiates through Kevlar windows (that are transparent to sound) into anechoic chambers on either side where individual microphones or microphone arrays are placed. The test section floor and ceiling are formed by Kevlar flow surfaces backed by acoustic absorbers and the facility is anechoic down to 180 Hz. Flow in the empty test section is closely uniform and of very low turbulence level (0.021% at 21 m/s). Further facility details are given by Devenport et al. [18].

The rotor used in this study is a left-handed 225% scale model of the rotor first used by Sevik [1], see Figs. 1 and 2. It has a diameter of 457 mm with a 127 mm hub. The rotor has 10 square tipped blades each with a chord of 57.2 mm. The blades are twisted from a pitch angle of 55.6° at the hub to 21.2° at the tips and have a thickness to chord ratio close to 9%. The design advance ratio is 1.17 and the zero-thrust advance ratio is 1.44 estimated using JavaProp [11].

In the study of wake ingestion from a cylinder, a 50.8-mm-diameter cylinder was mounted vertically in the test section 20 diameters upstream of the rotor disk, (see Fig. 1). The cylinder mounting allowed for its lateral position to be adjusted to vary the strike location of the wake center on the rotor. When the rotor yaw angle was changed, the lateral position of the cylinder was adjusted to maintain the same strike location on the rotor disk. Fences were placed on the cylinder 165-mm from the floor and ceiling to improve the two-dimensionality of its wake, verified using cross-sectional measurements with the rotor system removed [17]. All measurements were made for a fixed free stream velocity U_∞ of 20 ± 0.1 m/s corresponding to a Mach number of 0.057 and cylinder Reynolds number of 59,000.

3 Far-Field Sound Spectra

First, we will consider the results for the rotor ingesting the wake of the cylinder (Fig. 1). Figure 3a shows contours of sound pressure level (SPL) referenced at 20 μPa as a function of the advance ratio for a single microphone at receiver angle of 53° to the rotor upstream axis. These results are for the 100% starboard strike case where the cylinder axis is at the same lateral location as the starboard edge of the rotor and about half the rotor face was immersed in the wake. The dashed lines denote the blade passing frequency (BPF) and its harmonics. The far-field sound is characterized by broad haystacks centered around the blade passing frequency and its multiples due to the unsteady coherent loading on successive blades of the rotor. Haystacking is first seen for the blade passing frequency at an advance ratio of about 1.3 and becomes more pronounced as the advance ratio is reduced, appearing at about $J = 0.95$ for two BPF and at $J = 0.8$ for three BPF. Overall sound levels increase as the advance ratio is reduced because of the increase in rotor speed and the haystacking

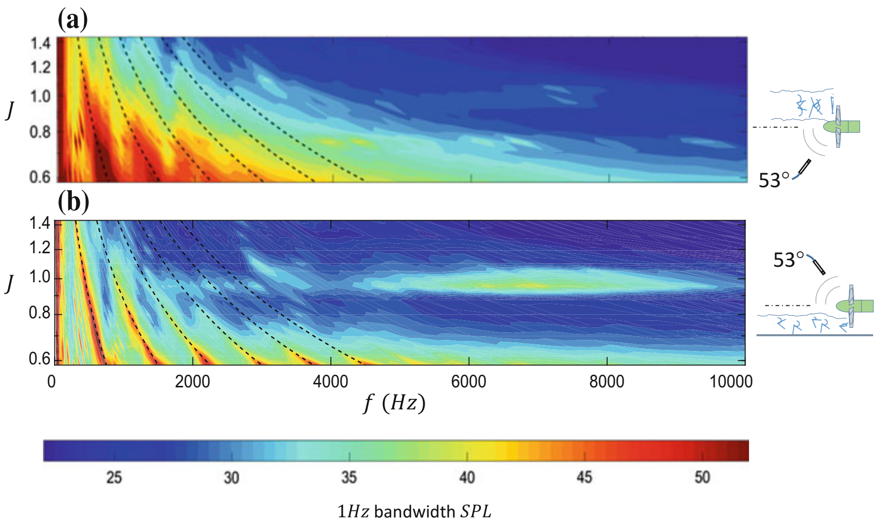

Fig. 3 Far-field noise spectra at an observer angle of 53° plotted as a function of advance ratio for the unyawed rotor. Dashed lines show the blade passing frequency and harmonics. **a** Wake ingestion, 100% starboard strike. **b** Boundary layer ingestion [12], with the rotor immersed in the top 80% of the boundary layer thickness δ, $\delta/R = 44\%$. Spectral levels scaled to an observer distance of 1.903 m

becomes more pronounced for the same reason—higher blade speed means a greater correlation between cuts of successive blades through the same turbulent eddy.

For comparison, Fig. 3b shows sound measurements of turbulent boundary layer ingestion into the same rotor from the study of Wisda et al. [12]. The horizontal ridge that is visible at frequencies of above 5 kHz for advance ratios around one is believed to be the result of trailing edge noise produced by coherent vortex shedding from the rotor blades, similar to that observed by Hersh et al. [19]. Spectral levels have been scaled to reflect the same observer radial distance as the wake measurement. As shown in the thumbnail sketch in Fig. 3b, the outer 1/3rd of the rotor radius is immersed in the boundary layer. Overall, sound levels caused by the boundary layer ingestion are substantially lower than those produced by the wake. There are two reasons for this; the boundary layer covers a significantly smaller portion of the rotor disk, and it is much less turbulent than the wake. Figure 4 compares mean velocity and turbulence profiles measured over the portion of the boundary layer swept by the rotor (in blue), with those measured in the wake. Despite having a higher mean velocity gradient, turbulence stresses in the boundary layer are 1/3rd to 1/6th of those in the wake, and thus upwash fluctuations experienced by the blades will be proportionately smaller. There are also detail differences between the wake and boundary layer ingestion. The sound spectrum for the boundary layer shows a much stronger trailing edge noise signature, the peak between 6 and 8 kHz and $J \approx 0.9$ (likely due to the much larger area of the rotor not exposed to turbulent inflow), and shows narrower more distinct

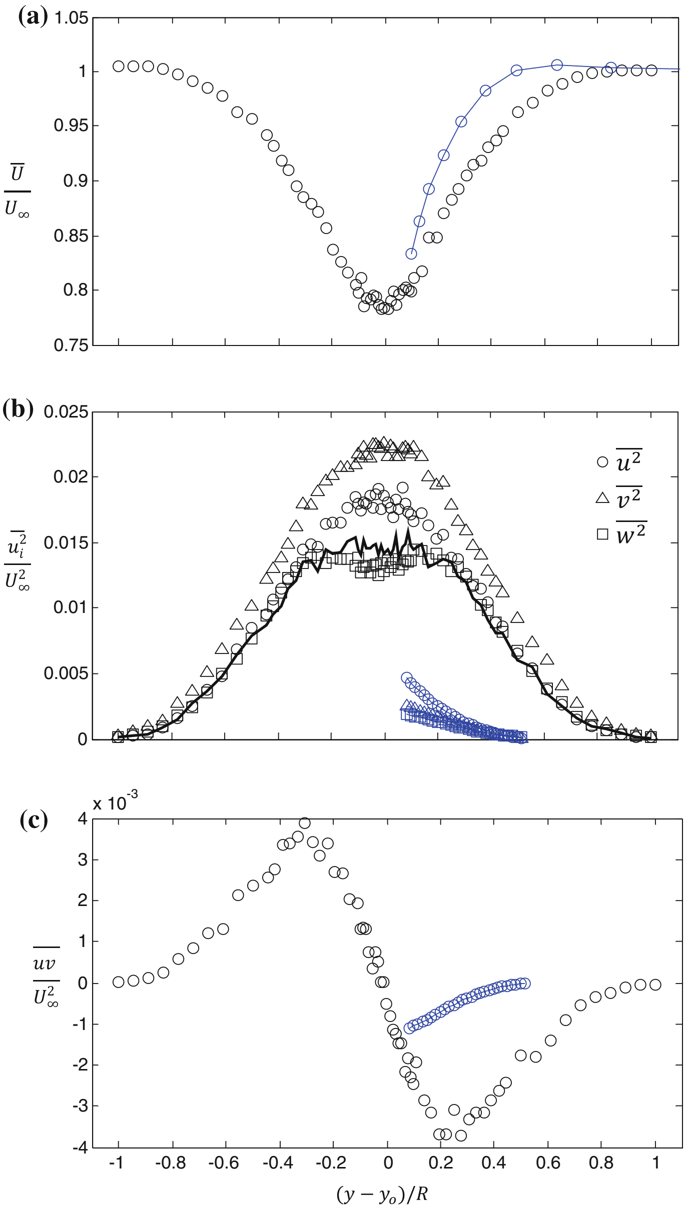

Fig. 4 Velocity profiles through the cylinder wake at $(x - x_{cyl})/D = 20$ (black markers) compared rotor-location boundary layer profiles from Morton et al. [9] (blue markers). **a** Mean velocity profile. **b** Reynolds normal stresses (solid black line shows $\overline{u^2}/U_\infty^2$ after high pass filtering at $fD/U_\infty = 0.015$). **c** Reynolds shear stress profile. Distances normalized on the rotor radius R

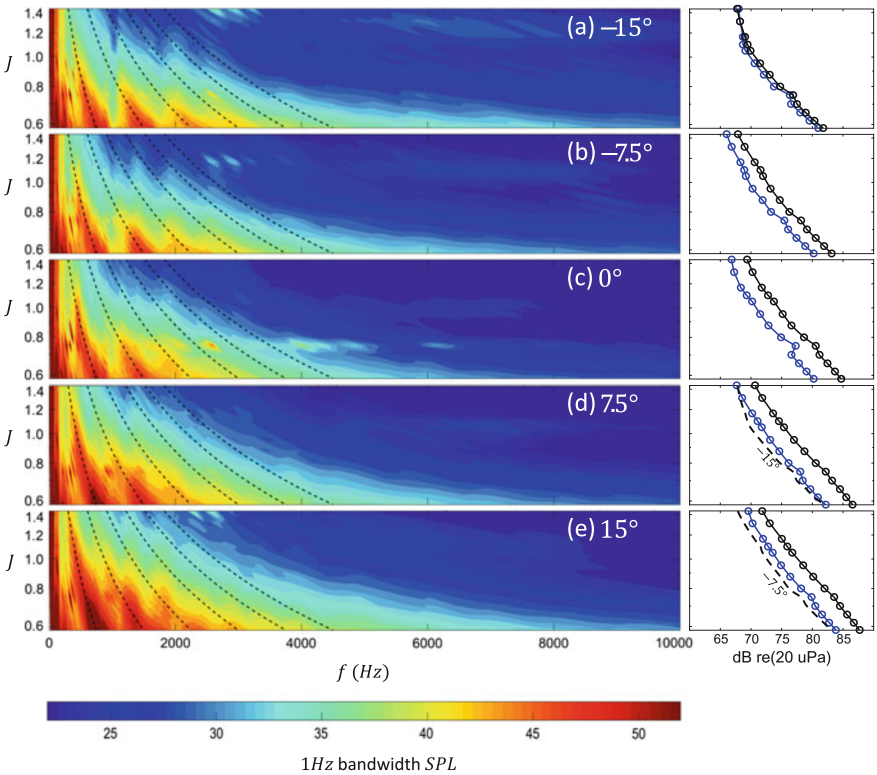

Fig. 5 Far-field noise spectra at an observer angle of 74° plotted as a function of advance ratio for different rotor yaw angles, 100% starboard strike. Dashed lines show the blade passing frequency and harmonics. Plots to the right of each contour set show OASPL as a function of advance ratio for observer angles of 53° (black) and 74° (blue) and use the same vertical axis as the spectral plots. Spectral levels scaled to an observer distance of 1.903 m

haystacks that extend to higher harmonics at a given advance ratio. The high level of the harmonics at high thrust was discussed in detail by Glegg et al. [15, 20] and is a consequence of the flow reversing direction near the wall at low advance ratios and causing clearly defined coherent structures, or an arch vortex system, that results in high sound levels caused by a blade-vortex interaction. These conclusions were substantiated by detailed PIV measurements made by Murray [21].

Figure 5 shows the effects of rotor yaw on the sound generated by wake ingestion for the same strike position as in Fig. 3. The spectral maps are shown for an observer angle of 74° to the rotor axis at -15, -7.5, 7.5, and 15° yaw. This figure includes plots (to the right) showing the variation of OASPL with advance ratio for both 53° (in black) and 74° (in blue), obtained by integrating over the frequency range from half the BPF to 20 times the BPF, capturing the full range of the broadband noise while eliminating background contamination at very low frequencies. As the rotor is yawed positively (Fig. 5c through e), overall spectral levels increase and the haystacks become less distinct. Negative yaw (Fig. 5a through c) produces the reverse effect. OASPL increases by about 6 dB from -15 to $15°$ yaw. The change in the degree of haystacking is likely due to the influence of yaw on the path taken by the rotor blades through the space-time correlation of the wake. The results suggest that there is a reduction of the blade-to-blade correlation with positive yaw. The change in overall sound levels can be explained in terms of directivity. If the sound directivity is fixed relative to the rotor axis, then a $-15°$ to $15°$ change in yaw angle changes the angle of a fixed observer measured from the rotor axis by the same amount. Assuming the rotor sound field to be directed primarily along the rotor axis, this results in an increase in sound levels with yaw. This equivalence between yaw and directivity holds quantitatively also. For example, an observer at $\theta = 53°$ is at an angle of $68°$ and $60.5°$ to the rotor axis for yaw angles of -15 and $-7.5°$, almost the same angles seen at $\theta = 74°$ for yaw angles of $7.5°$ and $15°$ and thus sees similar sound levels. This is shown in the OASPL plots of Fig. 5d and e where OASPLs measured at a receiver angle of $74°$ for yaw angles of $7.5°$ and $15°$ (blue curves) are compared with those measured at a receiver angle of $53°$ for yaw angles of -15 and $-7.5°$ (black dashed lines). Sound levels are the same, to within 1–2 dB.

4 Characteristics of the Undistorted Wakes

Figure 4 shows mean velocity and turbulence stress profiles through the undisturbed wake measured 20 cylinder diameters downstream without the rotor present. Also shown are the turbulence profiles for the boundary layer flow that impinges on the rotor when it is near the wall as shown in Fig. 2. The wake is almost symmetric with a maximum mean velocity deficit, Fig. 4a, of 22% and an overall width of approximately 2 rotor radii, just sufficient to immerse almost the entire rotor face when the projected centerline of the wake is on the rotor axis. The turbulence normal stress profiles (Fig. 4b) show levels to be quite high in the center of the wake with a peak intensity of about 14% in the v component. The anisotropy is evident here with normal-to-wake stress having the largest magnitude followed by the streamwise and spanwise stresses. The streamwise normal-stress profile is somewhat misleading as it includes contributions from some very low-frequency fluctuations. High-pass filtering at frequencies $fD/U_\infty > 0.015$ reduces streamwise turbulence levels to the profile indicated by the solid line, while having little discernable influence on the other stress components. We suspect that this is due to low-frequency flapping of the wake. Upwash measurements made in the rotor frame of reference, to be shown later, suggest that this motion may be stabilized when the rotor is installed. The Reynolds shear stress profile (Fig. 4c) appears closely antisymmetric, with a peak magnitude of about 0.004 U_∞^2.

Also shown in these plots are the corresponding results for the boundary layer flow, with the same outer mean flow (where y_o defines the wall location). While the mean flow deficit is similar, as shown in Fig. 4c, the turbulence stresses are much smaller in each case, as discussed above.

Figure 6 shows velocity correlation results for the wake and the boundary layer. Figure 6a shows streamwise integral length scales inferred from integral timescales and Taylor's hypothesis. The u component fluctuations have the longest streamwise scale of between 20 and 30% R (where R is the rotor radius) depending on position in the wake, whereas the integral scales of v and w are about half as large. Looking at the time delay correlation coefficient functions on the wake centerline, Fig. 6b, we see that v correlation function is oscillatory with a period close to $1.18\,R/U_\infty$ implying a Strouhal number, normalized on the cylinder diameter, fD/U_∞ of 0.19. This is therefore the coherent vortex shedding from the cylinder, and the streamwise integral scale in v is clearly much smaller than the true correlation distance because of the negative excursions in its correlation function. The u and w correlation functions have a much more monotonic form and decay to coefficients of 10% over timescales equivalent to streamwise distances of 90% and 20% R, respectively. The spanwise correlation coefficient functions measured at the wake center, Fig. 5c, show more uniform behavior among the three velocity components, with correlation coefficients falling monotonically to 10% over about one rotor radius in all cases.

Also shown in Fig. 6 are the corresponding results for the boundary layer flow normalized on the same parameters. First, we note that the lengthscale for the u component is similar to the lengthscale in the wake, but the lengthscales in the direction normal to the flow are much smaller for the boundary layer than in the wake when $(y - y_o)/R$ is about 0.5. This is also apparent when considering the spanwise scale shown in Fig. 6c, where the wake is clearly an order of magnitude more coherent in the spanwise direction than the turbulent boundary layer. This highlights the fundamental differences between these flows. In the case of the wake, the flow is clearly dominated by large turbulent structures that are of extended spanwise extent, whereas the boundary layer is more likely dominated by streamwise structures.

5 Turbulence Measurements in the Rotor Frame

The acoustic effect of decreasing advance ratio has been discussed above, but in order to predict the acoustic response of the rotor to the turbulent inflow, the distorted inflow itself must be known. An on-blade hotwire system as shown in Fig. 7 was used to measure this directly, particularly the unsteady upwash which is the dominant component of the unsteady blade loading. The data were phase-averaged to compute mean and unsteady velocity components as a function of blade angle. The phase-averaging was completed by dividing the blade rotation into one-degree bins.

Figure 8 shows the mean square unsteady upwash profile through the wake as measured by the on-blade hotwire at 90% radius with the cylinder at the center strike position (Note these measurements were made at 10 m/s rather than 20 m/s as used in the rotor noise tests). The profiles measured during the top and bottom passes through the wake are plotted separately as contours as a function of advance ratio,

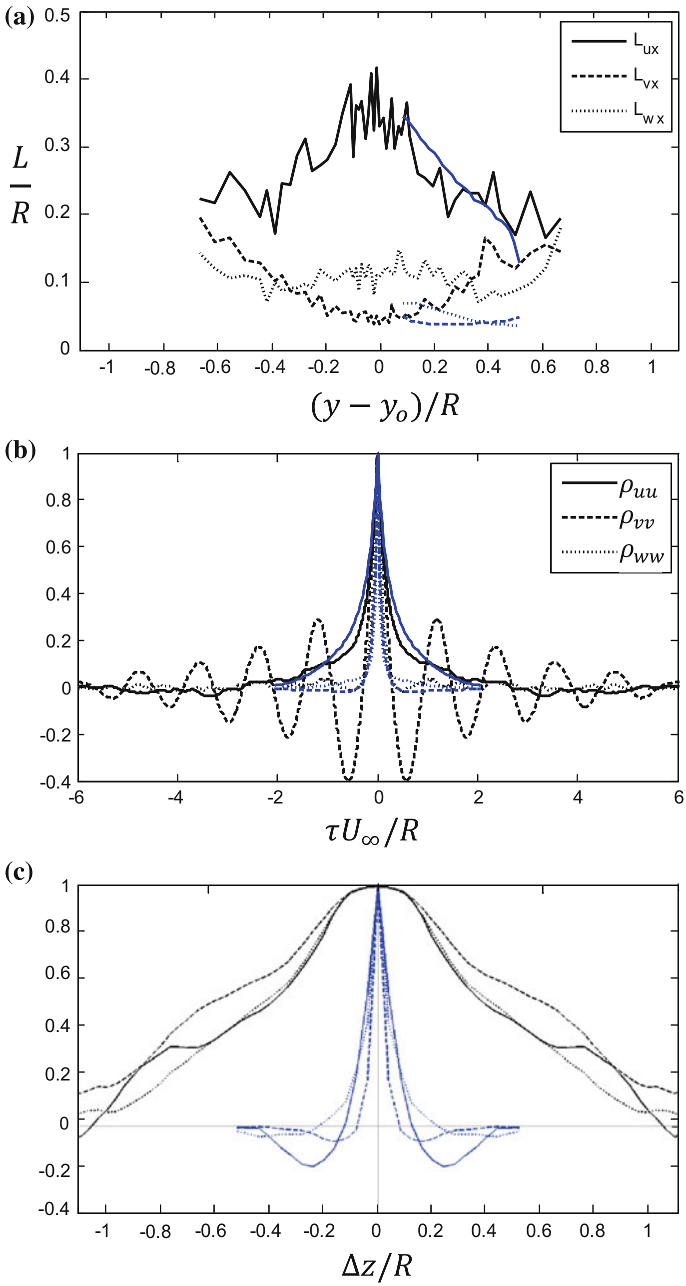

Fig. 6 Correlation statistics for the cylinder wake at $(x - x_{cyl})/D = 20$ (black markers) compared to rotor-location boundary layer profiles from Morton et al. [9] (blue markers). **a** Streamwise integral scale profile. **b** Time delay correlation coefficient functions, and **c** spanwise correlation coefficient functions at the wake center and 20% of the boundary layer thickness. Legend for part (**c**) is same as part (**b**)

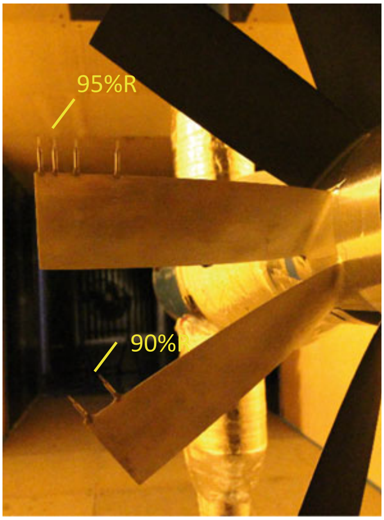

Fig. 7 View from upstream of the instrumented rotor blades showing the two probes for which results are reported

J. Note that profiles measured during the bottom pass appear shifted slightly (about 0.05 R) in the lateral direction compared to those measured during the top pass, but are otherwise very similar. This is not distortion. It is because the blade orientation is reversed during the two passes and thus the orientation of the upwash component is different. Because of the anisotropy of the wake turbulence structure, this results in a differently skewed profile. Distortion is apparent in the streamtube contraction that narrows the wake with increasing thrust and decreasing advance ratio. From $J = 1.44$ to 0.58, the width of the wake contracts by 16% before impact with the rotor face, but retains its roughly symmetric form. Note that peak upwash turbulence levels at low thrust (high J) are most similar to streamwise turbulence levels measured in the undisturbed wake (Fig. 4b) when low-frequency flapping motions are filtered out.

Figure 9 shows the unsteady upwash as seen by the probe at 90% radius, but in this case, the cylinder is at the 75% port strike location. Near zero-thrust, the center of the wake appears at the 75% R location as expected, but as the advance ratio decreases, the center of the wake is drawn across the rotor disk face toward its center, shifting by about 20% of the rotor radius at the lowest advance ratio. Comparing Figs. 8 and 9, it appears that the streamtube contraction is more drastic when the center of the wake is on the edge of the rotor disk, as might be expected from actuator disk theory. This difference impacts both the wake turbulence and the produced noise. For this single probe position, the relative velocity of the probe increases with decreasing advance ratio. One may expect the far-field noise from this particular blade strip to increase roughly as the sixth power of velocity (dipole source efficiency), but the observed changes, both distortion and wake movement, must also be considered when predicting the noise at a particular observer location. The dipole for this particular section of blade has a rotating directivity pattern. Movement in the center of the wake slides the peak radiative efficiency for this particular strip to another observer

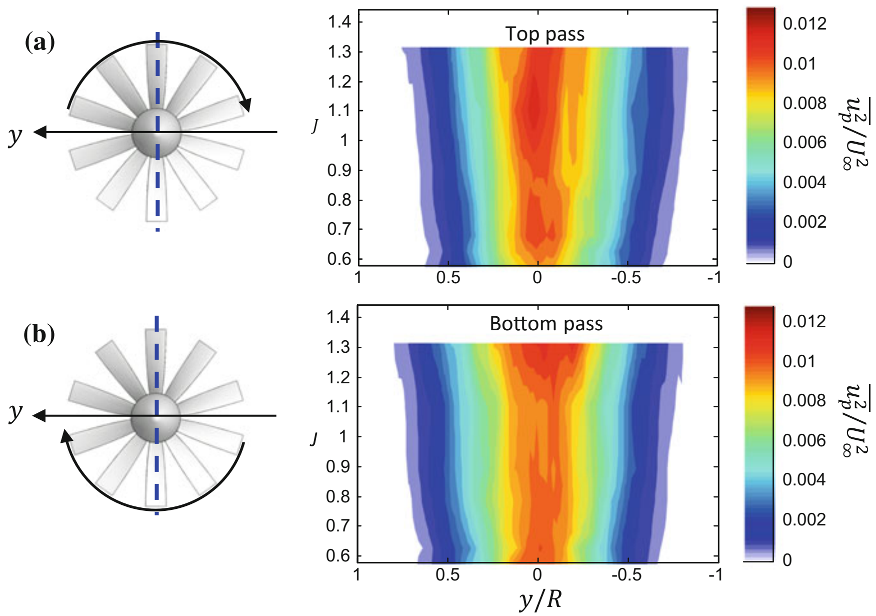

Fig. 8 Profiles of mean square upwash velocity seen at the 90% rotor radius as a function of advance ratio with the wake striking the center of the rotor. Profiles measured **a** during the top (positive z) pass, and **b** during the bottom pass

location. Of course, this effect will get integrated across the entire rotor disk in a full strip theory approach. Accurate prediction of the noise must fully account for this three-dimensional movement of the ingested wake even if the undisturbed wake could otherwise be considered two-dimensional and statistically stationary.

6 Rotor Noise Predictions

The noise levels from these rotor configurations were predicted using the method described by Glegg et al. [22]. In this approach, the far-field sound spectrum is predicted by considering the unsteady loading on each section of the blade. A strip theory approach is used and the spectral density in the far field is directly related to the cross-correlation of the unsteady loadings on each blade section and also between blades. To obtain the unsteady loading correlation, the blade response to an incoming gust is evaluated in the time domain. This allows the unsteady force correlation function to be directly related to the velocity correlation function of the unsteady inflow. The hotwire measurements by Morton [9] of the boundary layer flow and the measurements by Molinaro [23] of the wake provide the two-point correlation function in the detail required as an input to the code. This data set is

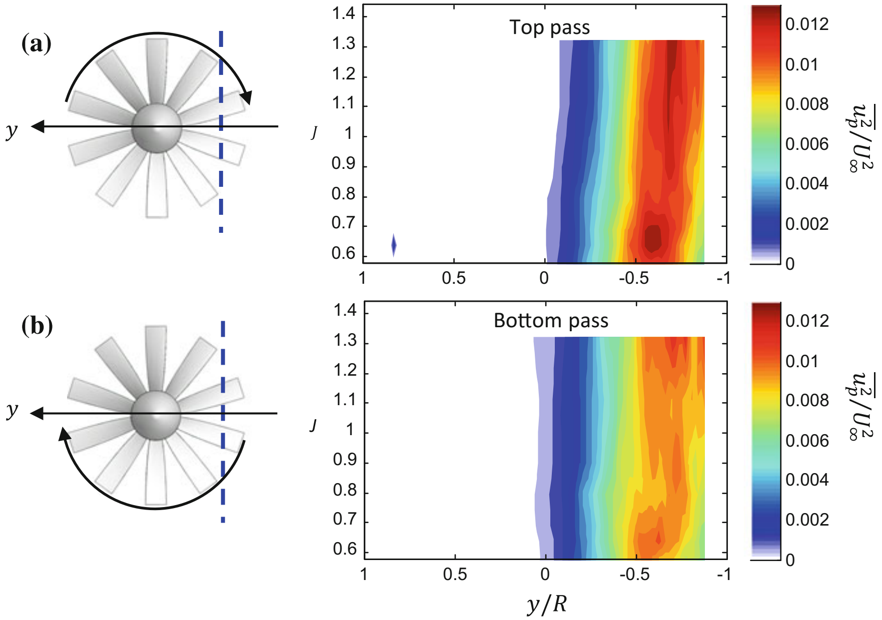

Fig. 9 Profiles of mean square upwash velocity seen at the 90% rotor radius as a function of advance ratio with the wake striking at the 75% port location. Profiles measured **a** during the top (positive) pass, and **b** during the bottom pass

not trivial since the correlation function is four-dimensional if Taylor's hypothesis is assumed. One of the added advantages of assuming Taylor's hypothesis is that the correlation function is defined as a function of time delay, which is exactly equivalent to the drift function of the local turbulent flow so the only correction required for the distortion as the turbulence enters the rotor is a small amplitude correction caused by the contraction of the stream tube. This amplitude correction is illustrated in Figs. 8 and 9 as a function of advance ratio and gives a correction to the far-field sound of only a fraction of a dB.

Using this approach, the predicted far-field sound spectra for various cases is illustrated in Figs. 10 and 11. The conclusion for these studies is that providing sufficient information about the inflow turbulence is available; then, rotor noise prediction can be quite accurate. The only significant error in the predictions shown in Figs. 10 and 11 is for the lowest advance ratio for the case of the rotor operating in the boundary layer (Case D, Fig. 10). However, this poor prediction is the result of the formation of a coherent, non-turbulent structure in the flow and is discussed in detail in [20] and in Sect. 3.

The results in Fig. 11 are for a yawed rotor and the predictions are based on the hypothesis that the inflow is unaffected by the yaw, and the main effect is the change in directivity cause by the relative position of the observer to the rotor axis.

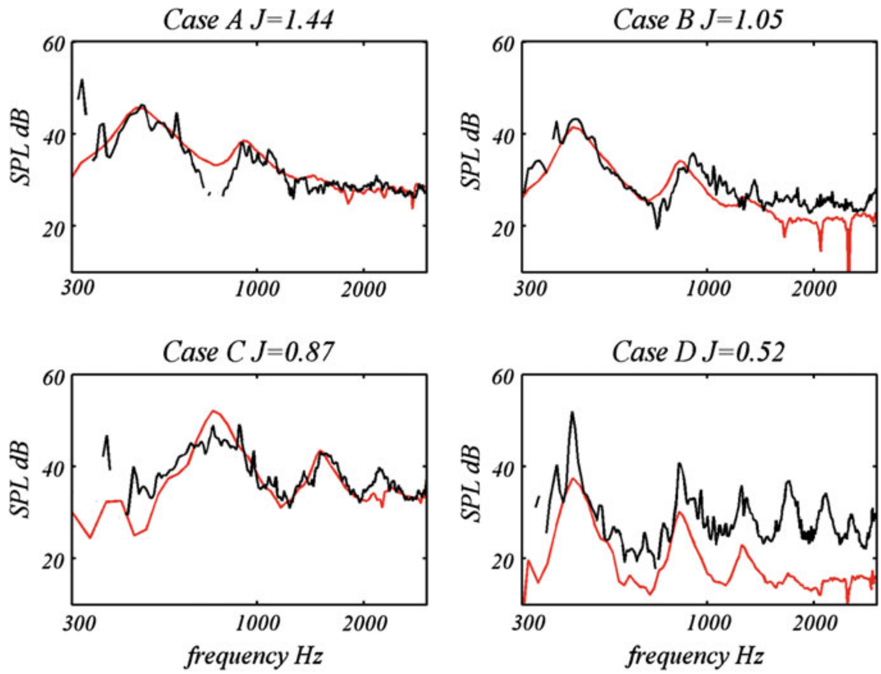

Fig. 10 Predicted (red) and measured (black) far-field sound spectra for the rotor operating in a wall boundary layer for a fixed microphone and at different advance ratios, see [15, 16]

This approach appears to work well for the case shown, and for all the other cases considered, as discussed in Sect. 3.

7 Conclusions

Measurements have been performed on a scaled version of a Sevik rotor ingesting both a planar turbulent wake and a turbulent boundary layer flow. In both cases, detailed measurements were made of the inflow turbulence, including three-component turbulence profiles and the full cross-sectional 4-dimensional space-time correlation function. Far-field sound measurements were also made of the turbulence ingestion noise for a comprehensive range of rotor advance ratios varying from zero to high thrust, for rotor yaw angles out of the plane of the wake from −15 to 15°, and for a range of wake strike positions on the rotor disk. Probes mounted on two of the rotor blades were used to measure upwash fluctuations seen in the rotating frame, as well as blade-to-blade coherence spectra. Comparisons have been made with predictions based on the measured inflow turbulence for both configurations and good results were obtained in all cases.

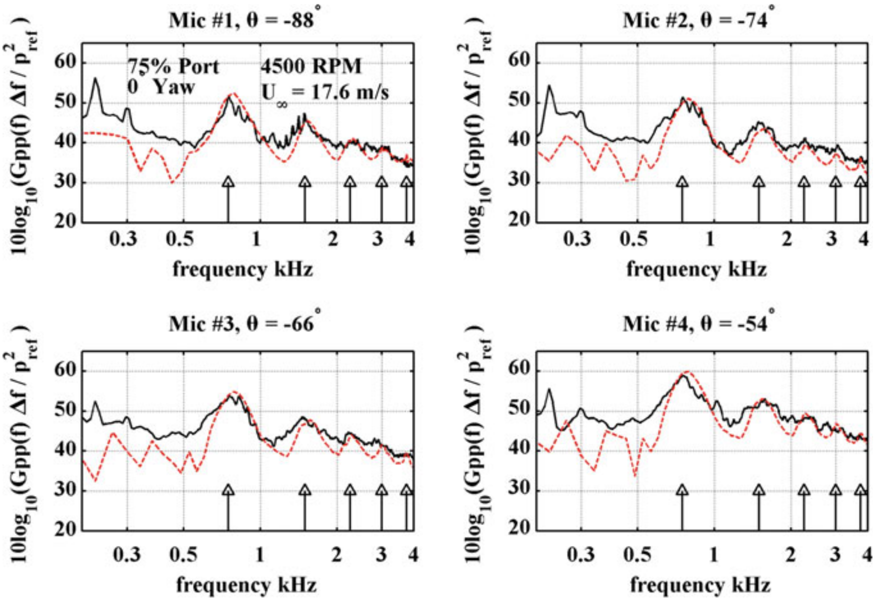

Fig. 11 Predicted (red) and measured (black) far-field sound spectra for the rotor operating in the wake of a cylinder for a fixed speed and different microphone locations

The wake was found to produce an intense and anisotropic turbulent inflow with a width approximately equal to the rotor diameter. Streamwise correlations at the rotor plane were found to be dominated by vortex shedding at a Strouhal number of 0.19, the train of eddies producing correlated velocity fluctuations over time delays equivalent to the passage of about 6 rotor radii. Correlations in the spanwise direction extended over about 1 rotor radius. Sound spectra measured with the rotor showed haystacking at the blade passing frequency and higher harmonics for a range of thrusting conditions produced by multiple cutting of the same turbulent eddies by successive blades. Compared to boundary layer ingestion, wake ingestion produced much louder sound, because of the higher wake turbulence levels and the greater area of the rotor disk immersed. With the boundary layer, however, the haystacks are more distinct and extend to higher harmonics. This is partly because the boundary layer eddies have a much smaller spanwise extent so that successive blade interactions with the large eddies are more impulsive and partly because of the reverse flow effects near the wall that cause the formation of a coherent vortex structure under the rotor.

Yawing the rotor in the wake produces some change in the definition of the haystacks, due to the change in the correlation structure of the turbulence cut by the blades, but the major effect is a change in overall sound levels. This change is a directivity effect, the sound field being determined primarily by the observer angle relative to the rotor axis rather than the flow axis.

On-blade hotwire measurements reveal the distortion of the wake as it is drawn into the rotor. With the center of the wake striking the center of the rotor, the principal effect of the distortion is the narrowing of the wake with increasing thrust due to streamline contraction. With the wake striking closer to the edge of the disk, the principal effect is the drawing of the wake toward the center of the rotor disk increasing the area of turbulence interaction.

Acknowledgements The authors would first like to thank Henry Murray, Ian Clark, and Anthony Millican for their assistance during the wind tunnel entries, and Mr. Michael Marcolini for his insightful observations and help with reviewing the manuscript. The authors would also like to thank the Office of Naval Research, in particular Dr. Ki-Han Kim and Dr. John Muench, for their support of this research through grants N00014-14-1-0141 and N00014-16-1-2395.

References

1. Sevik, M.: Sound radiation from subsonic rotor subjected to turbulence. In: International Symposium on Fluid Mechanics and Design of Turbo Machinery. University Park, Pennsylvania (1973)
2. Scharpf, D.F., Mueller, T.J.: An experimental investigation of the sources of propeller noise due to the ingestion of turbulence at low speeds. Exp. Fluids **18**, 277–287 (1995)
3. Minniti, R.J.I., Blake, W.K., Mueller, T.J.: Inferring propeller inflow and radiation from near-field response, part 1: analytic development. AIAA J. **39**, 1030–1036 (2001)
4. Minniti, R.J.I., Blake, W.K., Mueller, T.J.: Inferring propeller inflow and radiation from near-field response, part 2: empirical application. AIAA J. **39**, 1037–1046 (2001)
5. Wojno, J.P., Mueller, T.J., Blake, W.K.: Turbulence ingestion noise, part 1: experimental characterization of grid-generated turbulence. AIAA J. **40**, 16–25 (2002)
6. Wojno, J.P., Mueller, T.J., Blake, W.K.: Turbulence ingestion noise, part 2: rotor aeracoustic response to grid-generated turbulence. AIAA J. **40**, 26–32 (2002)
7. Ganz, U.W., Joppa, P.D., Patten, T.J., Scharpf, D.F.: Boeing 18-Inch Fan Rig Broadband Noise Test, in, NASA (1998)
8. Stephens, D.B., Morris, S.C.: Sound generation by a rotor interacting with a casing turbulent boundary layer. AIAA J. **47**, 2698–2708 (2009)
9. Morton, M.A., Devenport, W.J., Glegg, S.: Rotor inflow noise caused by a boundary layer: inflow measurements and noise predictions. In: 18th AIAA/CEAS Aeroacoustics Conference. Colorado Springs, Colorado (2012)
10. Alexander, W.N., Devenport, W., Morton, M., Glegg, S.: Noise from a rotor ingesting a planar turbulent boundary layer. In: 19th AIAA/CEAS Aeroacoustics Conference. Berlin (2013)
11. Wisda, D., Alexander, W.N., Devenport, W.J., Glegg, S.A.: Boundary layer ingestion noise and turbulence scale analysis at high and low advance ratios. In: 20th AIAA/CEAS Aeroacoustics Conference. Atlanta GA (2014)
12. Wisda, D., Murray, H., Alexander, N., Nelson, M.A., Devenport, W.J., Glegg, S.: Flow distortion and noise produced by a thrusting rotor ingesting a planar turbulent boundary layer. In: Aviation 2015. Dallas, TX (2015)
13. Murray, H., Wisda, D., Alexander, N., Nelson, M.A., Devenport, W.J., Glegg, S.: Sound and distortion produced by a braking rotor operating in a planar boundary layer with application to wind turbines. In: Aviation 2015. Dallas, TX (2015)
14. Alexander, W.N., Devenport, W.J., Wisda, D., Morton, M.A., Glegg, S.A.: Sound radiated from a rotor and its relation to rotating frame measurements of ingested turbulence. In: 20th AIAA/CEAS Aeroacoustics Conference. Atlanta, GA (2014)

15. Glegg, S., Buono, A., Grant, J., Lachowski, F., Devenport, W., Alexander, N.: Sound radiation from a rotor partially immersed in a turbulent boundary layer. In: Aviation 2015. Dallas, TX (2015)
16. Glegg, S., Grant, J., Wisda, D., Murray, H., Alexander, N., Devenport, W.: Broadband noise from a rotor at an angle to the mean flow. In: AIAA Scitech 2016. San Deigo, CA (2016)
17. Alexander, W.N., Molinaro, N.J., Hickling, C., Murray, H., Devenport, W.J., Glegg, S.A.: Phased array measurements of a rotor ingesting a turbulent shear flow. In: 22nd AIAA/CEAS Aeroacoustics Conference. Lyon, France (2016)
18. Devenport, W.J., Burdisso, R.A., Borgoltz, A., Ravetta, P.A., Barone, M.F., Brown, K.A., Morton, M.A.: The Kevlar-walled anechoic wind tunnel. J. Sound Vib. **332**, 3971–3991 (2013)
19. Hersh, A.A., Soderman, P.T., Hayden, R.E.: Investigation of acoustic effects of leading-edge serrations on airfoils. J. Aircr. **11**, 197–202 (1974)
20. Glegg, S., Grant, J., Murray, H., Devenport, W., Alexander, N.: Sound radiation from a rotor operating at high thrust near a wall. In: AIAA/CEAS 22nd Aeroacoustics Conference. Lyon, France (2016)
21. Murray, H.H.: Turbulence and Sound Generated by a Rotor Operating Near a Wall, MS Thesis. Aerospace and Ocean Engineering, Virginia Tech (2016)
22. Glegg, S.A.L., Devenport, W.J., Alexander, A.: Broadband rotor noise predictions using a time domain approach. J. Sound Vib. **335**, 115–124 (2015)
23. Molinaro, N.J.: The Two Point Correlation Structure of a Cylinder Wake, MS Thesis. Aerospace and Ocean Engineering, Virginia Tech (2017)